Collapse Accident Site Investigation using Terrestrial LiDAR Surveying

Jung Y.H. [1], Lim E.T.[1], Koo S.[1] and Kim S.S.[2*]

[1]Research, Disaster Scientific Investigation Division, National Disaster Management Research Institute, Republic of Korea

[2]Researcher Officer, Disaster Scientific Investigation Division, National Disaster Management Research Institute, Republic of Korea

*sskim73@korea.kr (*Corresponding author's email only)

Abstract **:** *A collapse incident is one of the representative disaster accidents. Collapses can occur due to internal defects during the design phase, but other collapses are caused by natural disasters such as typhoons or heavy rainfall, as many structures are exposed to the environment. Therefore, continuous inspections of structures are crucial. Additionally, investigating the causes and damages of already occurred collapse accidents is necessary for preventing recurrence and post-management. However, dealing with and investigating collapse sites is challenging due to the risk of additional collapses. To overcome these challenges, utilizing terrestrial LiDAR is suitable for conducting on-site investigations in secured locations. This study suggests the approach of using terrestrial LiDAR for collapse site investigations. Obtained scan data for the entire collapse site of Jeongja Bridge, which occurred on April 5, 2023, using terrestrial LiDAR. LiDAR measurements were performed at 13 locations to acquire data for the upper and side portions of the bridge. The acquired data was integrated to construct a single point cloud through registration. Additionally, mesh modeling was performed to create a model of the bridge. Using the generated bridge model, the slope of the upper part of the bridge was analyzed to visually identify the area where the bridge had sagged. Furthermore, the end length of the bridge model was measured, and cross-sections of the piers and abutments were extracted for a comparative analysis with design drawings, confirming the displacement of each part of the bridge. Therefore, through the 3D model constructed using terrestrial LiDAR, conducted visual inspection and surveying of the collapsed bridge without moving in the collapse site. In this study, confirmed the potential of using high-density terrestrial LiDAR in large-scale and high-risk structure collapse sites. It serves as a preliminary study for efficiently conducting investigations in challenging real collapsed sites.*

Keywords: Terrestrial LiDAR, Point cloud, Collapse accident, Disaster Investigation

Introduction

In South Korea, following the enactment of the Framework Act on the Management of Disasters and Safety in 2004, the terms "natural disaster," "man-made disaster," and "social disaster" were used. However, with the revision of the Act in 2014, the terms were standardized to "natural disasters" and "social disasters" (Kim et al., 2015). Natural disasters include commonly known events such as floods, typhoons, and strong winds, while social disasters encompass explosions, collapses, fires, and recent occurrences like the COVID-19 pandemic, the spread of animal diseases, and fine dust pollution. Disasters often occur suddenly before we become aware of them. While natural disasters such as typhoons and heavy rainfall can sometimes be predicted and warned about through extensive efforts, social disasters often arise unexpectedly. Particularly, accidents involving large-scale structures like bridges can result in significant loss of life and property.

Every year, the Ministry of the Interior and Safety in South Korea publishes statistical information on disasters. An analysis of the trend of social disasters over the past decade, from 2013 to 2022, indicates an increase in the last three years. In 2022, a total of 1,625 collapse incidents occurred, resulting in 197 casualties. While the most crucial aspect of disaster management is prevention, proper response to occurring disasters is paramount.

Collapse accidents are among the representative types of disaster accidents. While these can be caused by internal defects during the design phase, most structures are exposed to environmental factors, making them prone to failures due to natural disasters like typhoons and heavy rains. Therefore, ongoing inspections are crucial. In cases of structural collapse, not only are the human and property damages significant, but managing the aftermath is also challenging. When human casualties occur, nearby police, firefighters, and paramedics are the first to respond on the scene. They assess and spread awareness of the situation and conduct search and rescue operations for affected individuals.

However, the danger of such disasters is heightened by the fact that they can continue to pose risks even after the initial incident. Damaged structures that seem stable may suddenly collapse, causing secondary damage. This subsequent risk places significant constraints on the activities of police, firefighters, and paramedics responding to the disaster. From the moment a disaster strikes, firefighters working on search and rescue operations in the affected area are at constant risk of unexpected secondary disasters, which can lead to injuries or even loss of life. Hence, disaster sites are fraught with unforeseen dangers, necessitating considerable risk management.

To safely conduct investigations in the face of secondary disaster risks, utilizing three-dimensional spatial information that accurately replicates the disaster site can be an effective method. One such technology is LiDAR (Light Detection and Ranging), which uses thousands to millions of laser pulses per second to scan the surroundings. The scanning precision is high enough to create detailed 3D maps that capture not only the terrain and features but also human shapes. In outdoor areas where GNSS (Global Navigation Satellite System) reception is possible, coordinates can be obtained to determine surrounding positions, thus yielding highly reliable data.

Research is ongoing to leverage LiDAR technology across various fields. Lee and Jeon (2017) quantified rock joint roughness variables according to measurement intervals to assess the applicability of measuring rock slope joint roughness over large areas. Choi et al (2014) conducted a study to obtain point cloud data on the same plane using terrestrial LiDAR. Kang and Lee (2019) developed 3D spatial information for vertical structures using UAS (Unmanned Aerial System)-based image analysis and terrestrial LiDAR laser scanning, comparing positioning accuracy, completeness, and work efficiency. Jang (2006) compared the accuracy of land cover maps in agricultural areas using multispectral imagery and LiDAR data obtained from aircraft.

Recently, studies utilizing drone-mounted LiDAR to merge data with existing terrestrial LiDAR have also been actively conducted. Park and Hong (2022) performed a study on extracting land boundaries using drone LiDAR, and Lee and Suh (2022) discussed effective building modeling methods by using point cloud data-based indoor and outdoor building modeling with drone imagery, drone LiDAR, and terrestrial LiDAR.

This study aims to explore efficient ways to utilize terrestrial LiDAR in disaster site investigations. In April 2023, a collapse accident occurred on the Jeongja Bridge in Bundang-gu, Seongnam-si, where a portion of the cantilever structure's sidewalk section collapsed, causing casualties. This study involved surveying the Jeongja Bridge collapse site using terrestrial LiDAR and analyzing the acquired data to observe and analyze the bridge's current status, including the road surface and the gradient of both sidewalks. Through this, we aim to explore ways to utilize terrestrial LiDAR more effectively in disaster sites that pose unpredictable risks.

Research subjects and methods

a. Research subjects:

In April 2023, a collapse accident occurred at the Jeongja Bridge in Bundang-gu, Seongnam-si, South Korea. The Jeongja Bridge has a central fixed roadway, and the sidewalks on both sides are constructed in an unfixed cantilever structure. The cantilever structure, characterized by a beam supported on only one side, has become widely used with the development of construction technologies such as steel and reinforced concrete structures. While it is a useful structure commonly found in bridges, buildings, and even interior design, its stability requires regular inspections and maintenance.

According to the accident investigation report published by the Korea Authority or Land & Infrastructure Safety in South Korea, the direct cause of the collapse was identified as the loss of adhesion between the concrete directly beneath the road surface and the tensile reinforcement in the cantilever section. To discuss the applicability of terrestrial LiDAR in large-scale disaster sites, this study conducted data acquisition and analysis using terrestrial LiDAR at the Jeongja Bridge collapse site.

b. Research methods

In this study, the entire collapsed bridge was scanned using the Riegl VZ-2000 terrestrial LiDAR. The scan was conducted approximately 90 days after the accident occurred. Since debris from the collapse remained beneath the accident site, scanning was performed at 11 points around the site. From the top of the bridge, two points at the center of each side, where safety was ensured, were scanned, resulting in a total of 13 scan points. The VZ-2000 used in data acquisition was combined with a camera and GNSS receiver. To verify the positional accuracy of the acquired point cloud, three points on the bridge were separately measured and used as checkpoints. Data processing was performed using the dedicated software, RiSCAN Pro. Images were overlaid on the point clouds obtained from the 13 scan points, and all the data were matched. The positional accuracy of the terrestrial LiDAR data was verified using the previously mentioned checkpoints. Additionally, the overall shape of the bridge's road and sidewalk was modeled in 3D using the point cloud, and the detailed displacement was checked by comparing it with the design drawing.

c. Data acquisition and data processing

The Riegl VZ-2000 terrestrial LiDAR was used to acquire data from the collapsed bridge. The VZ-2000 was configured to be used with a Nikon D800 DSLR camera and Trimble R10 (Fig. 1), with their respective specifications as follows (Table 1). Therefore, the terrestrial LiDAR used in this study could acquire not only point cloud data but also imagery and positional information.

Table 1: Specifications for terrestrial LiDAR platform

Items	Details	
Trimble R10	Accuracy (Static)	Hor. 3mm+0.1ppm Ver. 3.5mm+0.4ppm
	Accuracy (RTK)	Hor. 8mm+1ppm Ver. 15mm+1ppm
Nikon D800 DSLR Camera	Resolution	3,630 megapixels
	Shutter speed	1/8,000 sec
Riegl VZ-2000 Scanner	Distance	Max. 2,050 (refic. 90%)
	Speed	Max. 396,000 pts/sec
	Range	Hor. 360

		Ver. 100
	Laser channel	Laser Class 1

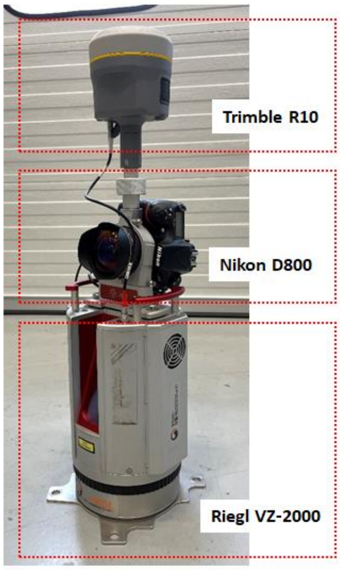

Figure 1: Terrestrial LiDAR(VZ-2000) combined with GNSS and camera.

The VZ-2000 can scan up to 2 km with very high precision. However, terrestrial LiDAR is highly affected by environmental factors, and data acquisition can be limited by obstructions around the target object, causing occlusion. When the entire target cannot be scanned from a single point, scans from multiple points must be performed and aligned. In this study, to compensate for these occlusion areas and acquire scan data for the entire bridge, scanning was conducted at 13 points in total (Fig. 0), and data alignment was performed using RiSCAN Pro software.

At each point, terrestrial LiDAR can acquire up to 5 photos according to the field of view (FOV). The point cloud is aligned with the imagery to construct the final point cloud, including image and positional information. The constructed point cloud was refined by removing noise generated during data acquisition and extracting the region of interest for 3D modeling.

Research results and analysis

To evaluate the positional accuracy of the processed data, the coordinates of three checkpoints were compared with those extracted from the generated point cloud (Table 4). The RMSE (Root Mean Square Error) for the terrestrial LiDAR checkpoints was found to be less than 0.020m, indicating a high level of accuracy.

Table 2: Comparison of coordinates between GNSS and Terrestrial LiDAR

Point	GNSS			Terrestrial LiDAR			Error		
	X(m)	Y(m)	Z(m)	X(m)	Y(m)	Z(m)	dX(m)	dY(m)	dZ(m)
C1	529920.470	209703.428	40.680	529920.457	209703.438	40.703	0.013	-0.010	-0.023
C2	529927.548	209617.160	40.799	529927.561	209617.144	40.817	-0.013	0.016	-0.018
C3	529912.479	209618.374	40.813	529912.494	209618.386	40.834	-0.015	-0.012	-0.021
RNSE(Root mean square error)							0.014	0.013	0.020

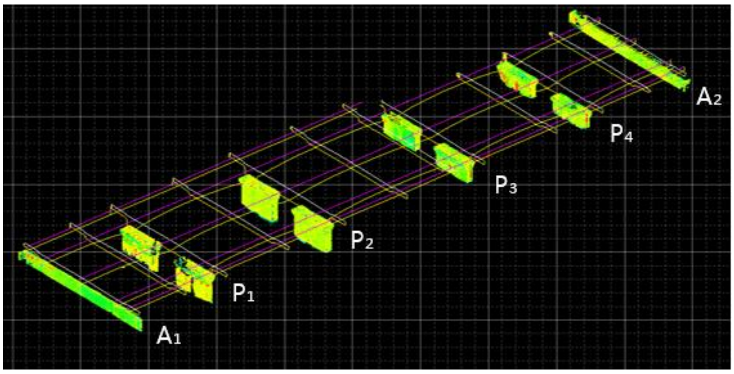

Figure 1: Cross section of bridge model.

With the high-accuracy point cloud established, a 3D mesh model was created to assess the overall condition of the bridge, including its upper and lower structures. Cross-sectional views of the bridge's abutments, piers, and intermediate sections were extracted from the generated model (Fig. 3). These cross-sections allowed for an observation of the bridge slab's condition at the abutments and piers (Fig. 4).

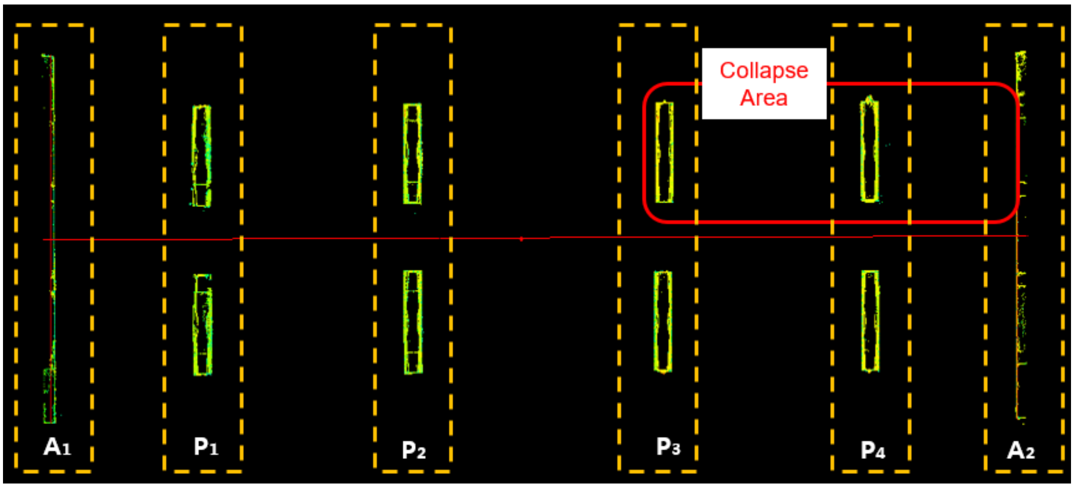

Figure 3: Bridge abutment and pier layout

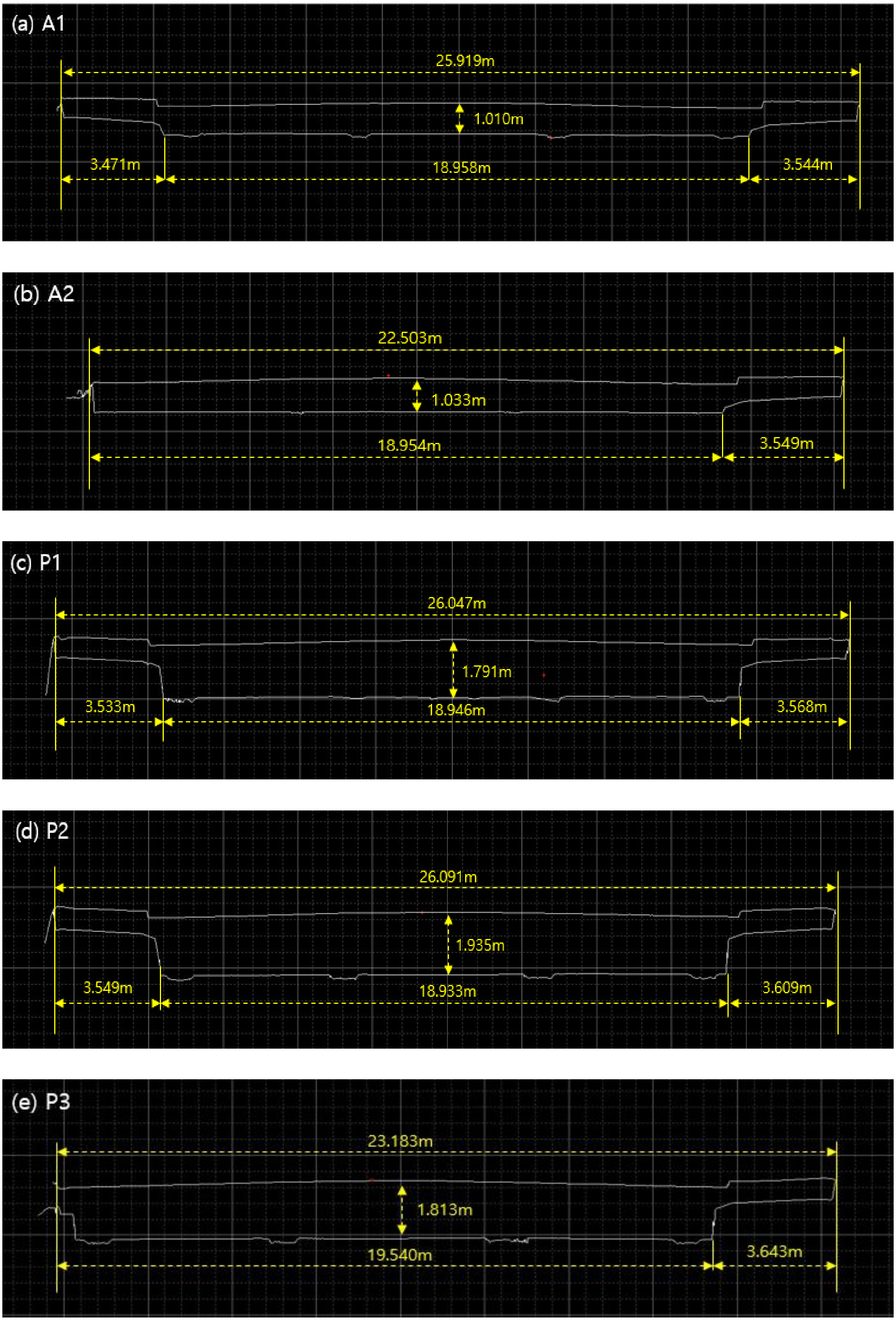

(a) A1
25.919m
1.010m
3.471m
18.958m
3.544m
(b) A2
22.503m
1.033m
18.954m
3.549m
(c) P1
26.047m
1.791m
3.533m
18.946m
3.568m
(d) P2
26.091m
1.935m
3.549m
18.933m
3.609m
(e) P3
23.183m
1.813m
19.540m
3.643m

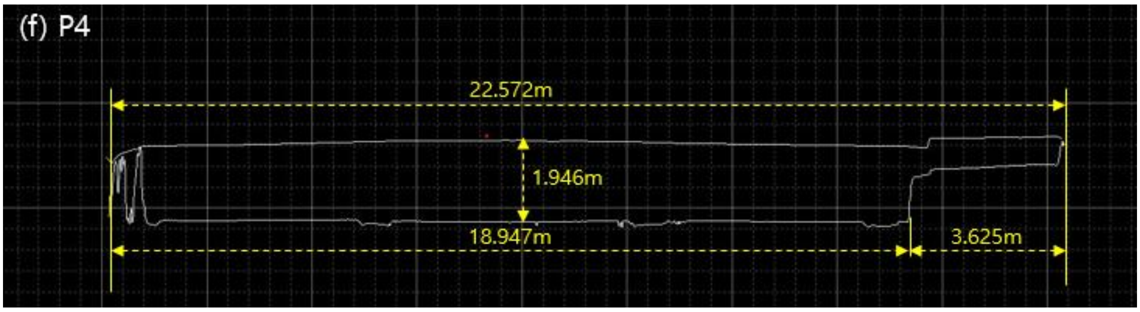

Fig. 4: Observation result of slab condition. (a) Abutment A1. (b) Abutment A2. (c) Pier P1. (d) Pier P2. (e) Pier P3. (f) Pier P4.

In Fig. 3, the pedestrian sections near the collapsed piers P3 and P4, and abutment A2 could not be assessed due to the collapse caused by the accident. However, the pedestrian section on the opposite side showed minimal differences. Observing the cross-sectional measurements of the pedestrian sections, the length on the left side where the collapse occurred, from A1 to P2, ranged from 3.471m to 3.549m. On the right side, from A1 to A2, the length ranged from 3.544m to 3.643m. Compared to the design plan, which specifies a sidewalk length of 3.5m, the left side showed a deviation of approximately -3cm to +5cm, while the right side showed a deviation of approximately +4cm to +14cm. The observed width of the bridge was between 25.919m and 26.091m, showing a deviation of about -2cm to +9cm from the design width of 26.000m. The measurements indicate that the left-side sidewalk, where the collapse occurred, was closer to the design specifications compared to the right side, and the overall width of the bridge exhibited only minor discrepancies from the design.

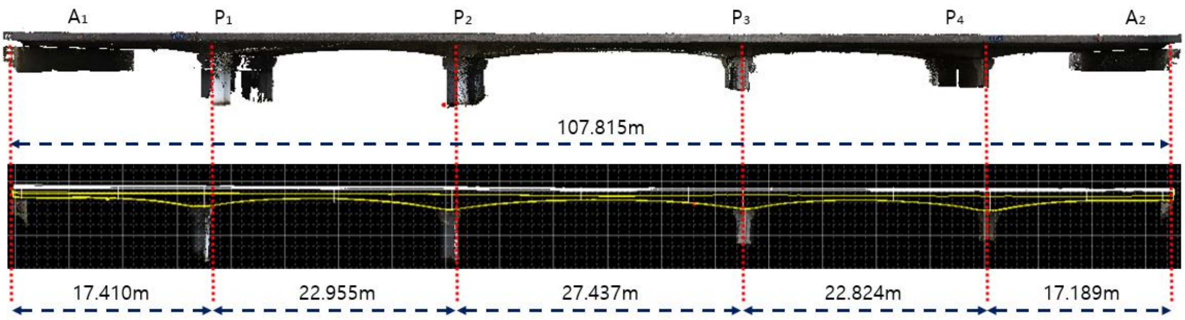

Figure 5: Observation of bridge side dimensions.

To assess the abutments, piers, and overall length of the bridge, the side view of the bridge was observed. Fig. 5 shows the side view of the bridge model. The distances from abutment A1 to A2, including the four piers (P1 to P4), were measured. According to Table 3, while there were slight variations at the endpoints and minor differences depending on the selection of the piers' central points, the overall measurements were found to be consistent. This consistency indicates that the bridge's structural components align well with the expected design, confirming the bridge's integrity in terms of length and positioning of its abutments and piers.

Table 3: Comparison of design distance and observation distance

	A1-P1	P1-P2	P2-P3	P3-P4	P4-A2	Total
Design distance(m)	17.450	23.000	27.000	23.000	17.470	108.000
Observation distance(m)	17.410	22.955	27.437	22.824	17.189	107.815
Difference value(m)	0.040	0.045	-0.437	0.176	0.281	0.185

To examine the road and sidewalk surfaces of the bridge, the point cloud data was modeled. For an accurate assessment of the surface slope, the collapsed section of the bridge was isolated, and the elevation values were represented as shown in Fig. 6.

This approach allowed for a detailed analysis of the bridge's surface inclinations, offering insights into the variations in slope, particularly around the collapse site. By visualizing the elevation changes, it was possible to understand the bridge's condition more comprehensively, highlighting any discrepancies or irregularities in the structure.

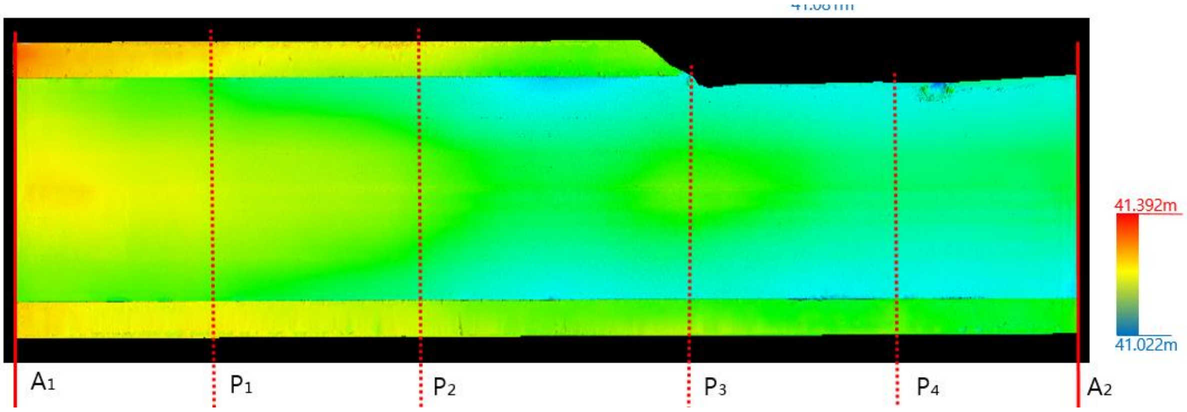

Figure 6: Bridge top view slope analysis.

Overall, it was observed that the abutment A1 at the top left of Fig. 5, where the collapse occurred, is elevated, and the elevation decreases towards the collapse site. Additionally, when comparing both sidewalks, the height of the sidewalk near the collapse site (the top of Fig. 7) is higher than that of the opposite side. The bridge's overall elevation ranges from approximately 41.02m to 41.39m.

Previously, the cross-sectional analysis indicated a thickness difference of about 2cm between abutments A1 and A2. This suggests that the ground level at the left side of Fig. 6, where abutment A1 is located, is higher than that at the right side, near abutment A2. This difference in elevation might have contributed to the structural variations observed in the bridge, offering a potential explanation for the collapse. The collapse of the Jeongja Bridge is attributed to the bond strength between the concrete at the base and the cantilever reinforcement. Therefore, in this study, the slope of both sidewalks of the bridge was observed. The sidewalks are designed with a 2% slope from the inside to the outside for drainage purposes.

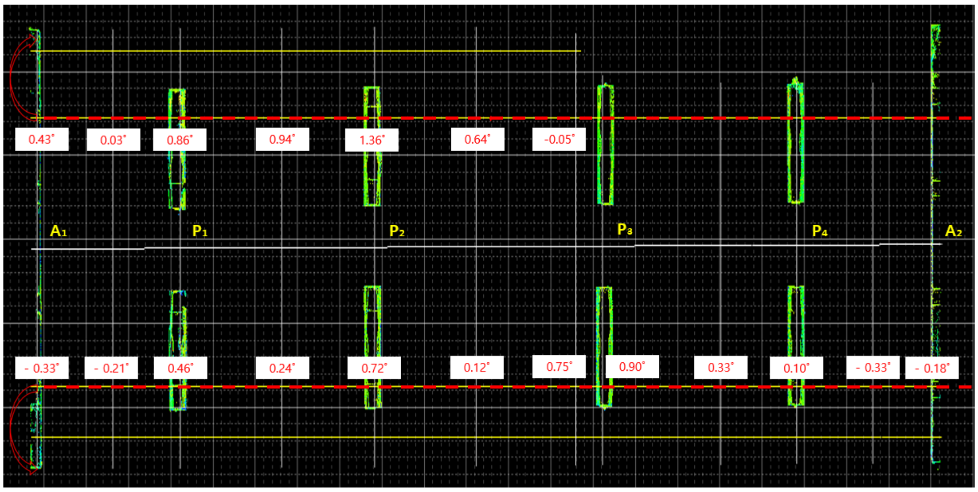

Figure **7:** Footbridges slope observation.

Observations from Fig. 7 reveal that the section on the right side, from P3 to A2, is collapsed and thus not available in the current data. Negative values in the observations indicate that the outer part of the sidewalk has sagged more than the inner part. Given that a 2% slope corresponds to approximately 1.15°, the data confirm that the outer part of the sidewalk has experienced a general downward displacement. Furthermore, it was noted that the section just before the collapse and the opposite abutments A1 and A2 experienced slightly more displacement compared to other areas.

This information provides insight into the structural changes and potential issues with the bridge's design, contributing to the understanding of the collapse mechanism.

Based on the cross-sectional, lateral, and plan views of the bridge, the comparison between the observed values at key points (excluding the collapsed area) and the design specifications shows only minor discrepancies. This suggests that the bridge was constructed in close accordance with the design drawings.

Conclusions

This study utilized terrestrial LiDAR to acquire data from a large-scale collapse accident site and analyzed the data to understand the current state of the collapsed bridge.

The results showed that the terrestrial LiDAR data had high positional accuracy, with an RMSE of less than 0.020m for the checkpoints. The overall shape of the bridge's road and sidewalk was modeled in 3D, and the detailed displacement was checked by comparing it with the design drawing. The analysis revealed that the collapsed section showed a significant height difference of approximately 30~50cm from the design state.

The study demonstrated that terrestrial LiDAR is an effective tool for disaster site investigations, especially for large-scale accidents where secondary disasters may occur. The technology can provide detailed and accurate 3D spatial information, which can be used to observe and analyze the current state of the disaster site. This information can help in the safe and efficient management of disaster sites, reducing the risks faced by first responders and aiding in the recovery process.

Overall, the study suggests that the use of terrestrial LiDAR in disaster site investigations can significantly enhance the understanding and management of such sites, contributing to improved safety and efficiency in disaster response and recovery efforts.

References

Choi.S.U., Choi.S.P., Jo.J.H., Kim.I.J. and Kim.U.N., (2014). *Automatic Technique for Adjustment error of Terrestrial LiDAR Data on Coplanar. Journal of the Korean Society of Cadastre, Volume 03-2014*

Jan.J.D., (2006). *Rural Land Cover Classification using Multispectral Image and LiDAR Data. Korean Journal of Remote Sensing, Volume 02-2006*

Kang.J.O. and Lee.Y.C., (2019). *Construction of 3D Spatial Information of Vertical Structure by Combining UAS and Terrestrial LiDAR. Journal of Cadastre & Land InformatiX, Volume 02-2019*

Kim.Y.G., Jang.H.S., Choi.Y.J. and Son.H.G., (2015). Disaster Classification for Optimal Disaster Response in Korea. *Journal of The Korean Society of Hazard Mitigation, Volume 06-2015*

Lee.J.G. and Suh.Y.C., (2022). *Indoor and Outdoor Building Modeling Based on Point Cloud Data Convergence using Drones and Terrestrial LiDAR, Journal of the Korean Society of Surveying, Geodesy, Photogrammetry and Cartography, Volume 06-2022*

Lee.S.D. and Jeon.S.K., (2017). *A Study on the Roughness Measurement for Joints in Rock Mass using LiDAR. Tunnel & Underground Space, Volume 01-2017*

Pack.J.C. and Hong.S.U., (2022). *Extraction Methods of Land Boundary using Drone LiDAR. Journal of the Korean Society of Cadastre, Volume 02-2022*